International Journal of Chemistry and Technology

http://dergipark.gov.tr/ijct

Research Article

Application of Sepiolite-Poly(vinylimidazole) composite for the removal of Cu(II): Thermodynamics and isotherm studies

Ali KARA[1,*] Muhsin KILIÇ[2], Nalan TEKIN[3], Nuray DINIBÜTÜN[1], Akif ŞAFAKLI[3]

[1]*Uludag University, Faculty of Arts and Science, Department of Chemistry, 16059 Bursa, Turkey*

[2]*Uludag University, Faculty of Engineering, Department of Machine, 16059 Bursa, Turkey*

[3]*Kocaeli University, Faculty of Arts and Science, Department of Chemistry, 41380 Kocaeli, Turkey*

Received: 03 October 2017, Revised: 01 February 2018; Accepted: 13 February 2018

*Corresponding author's e-mail address: akara@uludag.edu.tr (A. Kara)

ABSTRACT

For removal of Cu(II) ions from aqueous solutions, a novel composite was prepared from 1-vinyl imidazole and sepiolite by the technique of in-situ polymerization. Adsorption of Cu(II) ions onto Sepiolite-Poly(vinylimidazole) composite prepared has been studied at 277–338 K and the experimental data were analyzed using various isotherm models. The Langmuir and the Toth models procured the best fit to the experimental data of the adsorption among the two-parameter and three-parameter models, respectively. The adsorption equilibrium was reached in 3 h and the optimum pH for the adsorption was found to be 5. Adsorption isotherm modeling showed that the interaction between adsorbate and adsorbent is localized to monolayer adsorption. Maximum adsorption capacity (q_m) calculated from Langmuir isotherm was found to be 261.91 mg g^{-1} at 25^0C. The calculated thermodynamic parameters indicated an endothermic adsorption process. The composite is thought to be a promising adsorbent for the removal of Cu(II) ions.

Keywords: Sepiolite, composite, heavy metal, nonlinear isotherms.

Cu(II)'nin giderimi için Sepiolite Poly (vinylimidazol) kompozitinin uygulanması: Termodinamik ve izoterm çalışmaları

ÖZ

Sulu çözeltilerden Cu(II) iyonlarının giderimi için 1-vinyl imidazole ve sepiyolit kullanılarak in-situ polimerizasyon yöntemi ile yeni bir kompozit hazırlandı. Hazırlanan Sepiolite-Poly(vinylimidazole) kompoziti üzerine Cu(II) iyonlarının adsorpsiyonu 277–338 K sıcaklık aralığında çalışıldı ve deneysel veriler çeşitli izoterm modelleri kullanılarak analiz edildi. Langmuir ve Toth modelleri, sırasıyla iki parametreli ve üç parametreli modeller arasındaki adsorpsiyonun deneysel verilerine en iyi uyumu sağlamıştır. Adsorpsiyon dengesine 3 saatte ulaşıldı ve adsorpsiyon için optimum pH' nın 5 olduğu bulundu. Adsorpsiyon izoterm modellemesi adsorbat ve adsorban arasındaki etkileşimin tek tabakalı adsorpsiyonla sınırlandırılmış olduğunu gösterdi. Langmuir izoterminden hesaplanan maksimum adsorpsiyon kapasitesinin (q_m) 25^0C'de 261.91 mg g^{-1} olduğu bulundu. Hesaplanan termodinamik parametreler endotermik bir adsorpsiyon prosesine işaret etti. Hazırlanan kompozitin Cu(II) iyonlarının giderimi için umut verici bir adsorban olduğu düşünülmektedir.

Anahtar Kelimeler: Sepiolite, kompozit, ağır metal, nonlinear izotermler.

1. INTRODUCTION

Heavy metal contamination is dangerous for ecological systems and living species due to their high toxicity and non-biodegradability.[1] Copper is a heavy metal, and is used for different applications such as stabilizers, pigments, paints, mining, pesticides, fertilizers, electro-plating and catalysts.[2] Copper can cause health problems such as gastrointestinal disturbance, Wilson's disease and lesions in the central nervous system at higher level.[3] Therefore, the removal of copper from wastewater and water resources is important to protect the environment and human health.

For the removal of copper in wastewaters, there are various common methods used such as chemical precipitation, oxidation–reduction, ion exchange, membrane filtration, flocculation, electrocoagulation, liquid–liquid extraction, electrodialysis and adsorption.[4,5] Among the conventional techniques, the adsorption process is mainly preferred due to its highly selective, easy handling, high efficiency, flexibility in design, avoidance of chemical sludge and wide availability of

different adsorbents.[6,7] Thus, effective and low-cost adsorbents for removing heavy metal ions from waste waters need to be developed. In recent years, various adsorbents have been widely used for the removal of Cu(II) from wastewaters.[8-15]

Clay-polymer composites have been considered as highly promising materials for many applications due to their unique properties such as thermal and mechanical stability, high particle dispersion, fire retardant, gas permeability and structural flexibility.[16] Clays are chosen as fillers for clay/polymer composites due to excellent chemical stability and large specific surface areas.[17] Although a few studies are reported on the removal of heavy metal ions by using clay-polymer composites, to the best of our knowledge, there is no report on the use of Sepiolite-Poly(vinylimidazole) (Sep-PVI) composite for removal of Cu(II).

Imidazole is a base and proton accepting monomer. Among imidazole-containing polymers, poly (vinylimidazole) (PVI) is used in prevalent studies because its imidazole groups have complexing properties with catalytic divalent metallic ions[18,19], besides antimicrobial activity and biodegradability[20,21] and low cost.[19] Sepiolite involves a continuous two-dimensional tetrahedral sheet and is a phyllosilicate, so the structure of sepiolite differs from other layer silicates.[22] The discontinuity of the silica sheets arises to the presence of silanol groups (Si–OH) at the tunnels edges. Hence sepiolite has a high specific surface area (> 300 m^2 g^{-1}) because of the tunnels in this structure. Therefore the interaction of interfacial between polymer and sepiolite enhances because of existence of silanol groups (Si–OH). Therefore, for the composite synthesized, the good dispersion of sepiolite within the polymer and improving of the mechanical and thermal properties are expected.[17-23]

The equations of adsorption equilibrium isotherm elucidate the adsorption process at the equilibrium conditions for an adsorption process or solid-liquid adsorption system.[24] From these adsorption isotherms, Freundlich and Langmuir isotherm models are the mostly used isotherms. The linear regression has been substantially used to estimate the parameters of the isotherm model in the literature. But, a transformation to linear form from nonlinear isotherm equations causes usually to culminate in the difference between experimental and theoretical data. Hence this result leads to deflect the fit in linear plots.[25] A nonlinear isotherm method is more suitable to obtain the parameters of the adsorption equilibrium isotherm.[26]

In the present work, Sep-PVI composite samples were synthesized by in situ polymerization. For the preparation of the composite, sepiolite was used without any chemical treatment as reinforcement filler. The characteristics of Sep-PVI composite were examined with various instrumental analyses such as differential scanning calorimetry (DSC), X-ray diffraction (XRD), scanning electron microscope (SEM), and Fourier transform infrared spectroscopy (FTIR). The Sep-PVI composite was also used to removal of Cu(II) ions from aqueous solution. The adsorption of Cu(II) onto the Sep-PVI composite has been investigated under various conditions such as temperature, type of adsorbent and initial solution concentration. Additionally, non-linear isotherm methods were used to evaluate the parameters of the adsorption isotherm model of Cu II) onto Sep-PVI composite.

2. MATERIALS AND METHOTDS

2.1. Materials

Sepiolite was obtained from Aktaş Lületaşı Co., Eskişehir-Turkey. The chemical composition of the sepiolite consists of 53.47 % SiO_2, 23.55 % MgO, 0.71 % CaO, 0.43 % NiO, 0.19 % Al_2O_3, 0.16 % Fe_2O_3, and it exhibits a 21.49 % loss on ignition from XRF measurement. From the BET analysis, the specific surface area was 342 m^2 g^{-1} for sepiolite.[27] Azobisisobutyronitrile (AIBN) and 1-vinyl imidazole (VIM) were purchased from Fluka and Aldrich, respectively. Copper (II) nitrate trihydrate was supplied from Fluka (Hannover, Germany). All other chemicals used this study were procured from Merck (Darmstadt, Germany) and were of reagent grade.

2.2. Synthesis of Sep-PVI composite

The clay sample was sieved to size fraction of 75 µm, dried at 105°C in an oven for 24 h and then used for the preparation of composite, and for the adsorption experiments. In this work, Sep-PVI composite was synthesized through in situ polymerization. Firstly, 0.16 g AIBN, 10 mL 1-vinylimidazole, calculated sepiolite (sepiolite content in polymer matrix is 2.5 % wt.), and 10 mL deionized water were mixed in the flask. For good dispersion of sepiolite, the suspension prepared was agitated vigorously for 3 hours by using the ultrasonic bath. After the preparation of the suspension, N,N'-methylenebisacrylamide (0.2 g) was added the mixture. The mixture was then heated to 65°C in a water bath for 200 min at under nitrogen atmosphere. The synthesized composite was washed with excessive deionized water. After the cleaning, the Sep-PVI composite was dried and ground to powder form.

2.3. Characterization of the composite

XRD patterns of the samples were recorded on a Rigaku Ultima IV X-ray Diffractometer. The experimental conditions were copper K alpha (CuKα) radiation generated at 40 kV voltages, 30 mA current and a scan speed of 1°/min. For FTIR experiments, IR spectra of the samples were recorded by a Bruker Tensor 27

spectrophotometer. The spectra were obtained by using Diamond ATR in the range of 4000–400 cm^{-1}, with a 2 cm^{-1} resolution over 30 scans. The thermal properties of the composite were studied by using a DSC (Perkin Elmer DSC 4000) at a heat rate of 10°C min^{-1} between room temperature and 1000°C. The surface morphology of the samples was investigated by SEM-EDX (JOEL 50 A) microscope including operations at 10 kV accelerating voltage. The surfaces of the samples were sputter-coated with gold before analysis.

2.4. Batch adsorption experiments

The adsorption experiments were carried out stirring in a beaker at 200 rpm by using a magnetic stirrer. The contact time to reach equilibrium was determined as 3 h.. 50 mL of 100 mg l^{-1} stock Cu(II) ions solution and 0.1 g of dried sample of Sep-PVI composite were used for the all adsorption experiments. The pH effect on the Cu(II) ion adsorption capacity of Sep-PVI composite was investigated in the pH range between 2.0 and 6.5. The further adsorption experiments were performed at 277, 298, 318, and 338 K at an optimum pH value of 5.0.. After the adsorption equilibrium, the supernatants were separated from the suspension by centrifugation for 5 min at 4500 rpm, and Cu(II) ions were analyzed by using an UV-vis spectrophotometer (Shimadzu-2100 UV-Vis, Japan). The adsorption capacity was calculated according to the following equation:

$$q_e = (C_0 - C_e)\frac{V}{m} \quad (1)$$

where, m (g) is the mass of the dried adsorbent, C_0 and C_e are the initial and equilibrium concentrations (mg l^{-1}) of Cu(II), V (l) is the volume of the Cu(II) solution and q_e (mg g^{-1}) is the adsorption capacity.

The non-linear isotherm models were evaluated by using the Cu(II) solutions ranging from 100 to 1000 mg l^{-1} at temperatures of 277, 298, 318, and 338 K for the adsorption.

3. Theory

3.1. Single- and two-parameter isotherms

According to Henry's law, the number of active sites is much higher than the number of solute molecules.[28] The adsorption isotherm equation is expressed by Eq. (2) (Table 1), where K_{HE} (l g^{-1}) is Henry's constant and C_e is Cu(II) equilibrium concentration (mg l^{-1}).

The Freundlich isotherm equation[29] is used for the definition of multilayer adsorption. This equation is given as by Eq. (3) Table 1, where, K_F is the constant of Freundlich isotherm representing adsorption capacity. n is the adsorption intensity, C_e is the equilibrium concentration (mg l^{-1}) of Cu(II) ions, and q_e (mg g^{-1}) is the amount Cu(II) ions adsorbed per unit of the composite (namely, adsorption capacity of the composite). If the value of n is between 1 and 10, the adsorption is suitable.[30]

The Langmuir isotherm model describes monolayer adsorption.[31] The Langmuir isotherm is given by Eq. (4) (Table 1), where, K_L (l g^{-1}) is the equilibrium constant related to the adsorption enthalpy by means of the van't Hoff equation, C_e (mg l^{-1}) is the equilibrium Cu(II) concentration in the solution, q_e (mg g^{-1}) is adsorption capacity of the composite and q_m (mg g^{-1}) is the monolayer adsorption capacity of the composite.

The Dubinin–Radushkevich isotherm supposes that the energy of adsorption is homogeneous on the surface of the adsorbent and the adsorption curve is related to the porous structure of the adsorbent.[32] In Eq. (5) (Table 1), where T is absolute temperature (K), R is the gas constant (8.314 J mol^{-1} K^{-1}), ε is Polanyi potential and it was calculated by using RT ln (1 + 1/Ce) equation, q_m is the D–R isotherm constant and C_e is the equilibrium Cu(II) concentration in the solution (mg l^{-1}). B is a constant which related to the adsorption energy. The value of E is calculated from $E = 1/\sqrt{2B}$ and the equation can be used to determine of the adsorption type.[33]

The Temkin isotherm model assumes that the heat of the adsorption of the adsorbate molecules would decrease linearly with coverage due to the adsorbent and adsorbate interactions.[30-33] It is presented by Eq. (6) (Table 1), in this equation, b is the variation of adsorption energy (J mol^{-1}), T is the temperature (K), $B_1 = RT/b$ is related to the adsorption heat, R is the universal gas constant (J mol^{-1} K^{-1}) and K_T is the equilibrium binding constant (l mg^{-1}) related to the maximum binding energy.

The Halsey isotherm model is used to confirm the heteroporous nature of the adsorbent and suitable for multilayer adsorption.[34] It can be given by Eq. (7) (Table 1), where q_e (mg g^{-1}) is adsorption capacity of the composite, K_H is the Halsey isotherm constant, n_H is the Halsey isotherm exponent and C_e (mg l^{-1}) is equilibrium concentration of Cu(II) ions in the solution.

3.2. Three-, four- and five-parameter isotherms

The Redlich-Peterson isotherm[35] model can be applied to both of homogenous and a heterogeneous system for a wide concentration range and it combines the properties of the Freundlich and Langmuir isotherms in a single equation. The isotherm equation is displayed by Eq. (8) (Table 1), in this equation, β is an exponent and the value of the exponent lies between 0 and 1, and K_R and a_{RP} are the constants of isotherm model (L mg^{-1}). If β = 0, it becomes the Henry's law and if β = 1, the isotherm equation turns out to the Langmuir isotherm equation.

The Sips isotherm[36] is a unification of the Langmuir and Freundlich isotherms. For low adsorbate concentrations, this isotherm equation reduces to the

Freundlich isotherm. The Sips isotherm equation foresees a monolayer adsorption capacity characteristic of the Langmuir isotherm at high adsorbate concentrations.[37] The isotherm equation given by Eq. (9) (Table 1), where K_s is the constant of Sips isotherm (l g^{-1}), q_m (mg g^{-1}) is the monolayer adsorption capacity of the composite, and γ is the model exponent of Sips isotherm.

The Khan isotherm model[38] is suggested to the pure solutions.[37] The isotherm model can be expressed by Eq. (10) (Table 1), in this equation, a_K and b_K are the exponent of the isotherm model and the constant of Khan model, respectively. Maximum adsorption capacity, q_m is predicted by the model with the correlation coefficients. If a_K equals to 1, Eq. (10) turns into the Langmuir isotherm. When $b_K C_e$ value is much bigger than unity, Eq. (10) can be turns into the Freundlich isotherm.[39]

The Radke-Prausnitz isotherm[40] can be given by Eq. (11) (Table 1), where r_R and a_R are the constants of Radke–Prausnitz model, and β_R is the exponent of Radke–Prausnitz isotherm.

The Toth model[41] is a special type of the Langmuir isotherm and convenient in defining heterogeneous adsorption.[37] It is given by Eq. (12) (Table 1), where b_T is the constant of Toth model and n_T is the exponent of Toth model and is associated with surface heterogeneity. If n_T is unity, the isotherm reduces to the Langmuir equation.

The Koble–Corrigan isotherm[42] incorporates the Freundlich and Langmuir isotherm models to point out the adsorption equilibrium data. It can be given by Eq. (13) (Table 1), where B_{KC}, A_{KC} and n_{KC} are the constants of Koble–Corrigan isotherm model. When the adsorption experiments carried out at high adsorbate concentrations, the isotherm model approaches the Freundlich isotherm.[43]

The Fritz and Schlunder model (four-parameter) developed to empirically four-parameter equation which is another form of Langmuir–Freundlich type isotherm model. The equation of this model expressed by Eq. (14) (Table 1), where B and A are the parameters of Fritz–Schlunder model, and α_{FS} and β_{FS} (α_{FS} and $\beta_{FS} \leq 1$) are the exponents of Fritz–Schlunder equation. For $\alpha_{FS} = \beta_{FS} = 1$, Eq. (15) reduces to the Langmuir equation and $K_L = B_{FS}$ is also the Langmuir isotherm constant (l mg^{-1}) related to the adsorption energy and $A = K_L q_m$.[45]

The Fritz–Schlunder model (five-parameter) represents a wide field of equilibrium data through the five-parameter empirical expression.[44] It can be given by Eq. (15) (Table 1), where α_1, α_2, α', β_1 and β_2 (β_1 and $\beta_2 \leq 1$) are the Fritz–Schlunder parameters. When the exponent's β_1 and β_2 are equal to unity, the isotherm model reduces to Langmuir model and approaches the Freundlich model for higher liquid phase concentrations.[43]

4. RESULTS AND DISCUSSION

4.1. Characterization of the Sep-PVI composite

The Sep-PVI composite was synthesized by in situ polymerization of sepiolite which was used without any chemical treatment and vinyl imidazole (VIM). The synthesis process was given in Scheme 1.

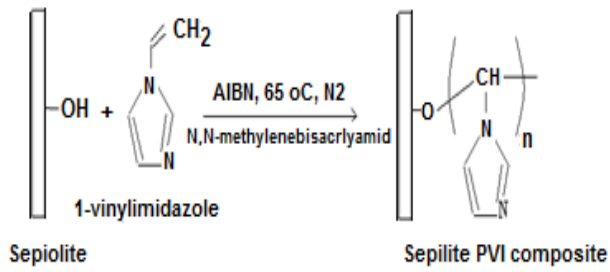

Scheme 1. The formation process proposed for Sep-PVI composite.

4.1.1. FTIR analysis

The FTIR spectra of Sep-PVI composite, PVI and sepiolite are given in Figure 1.

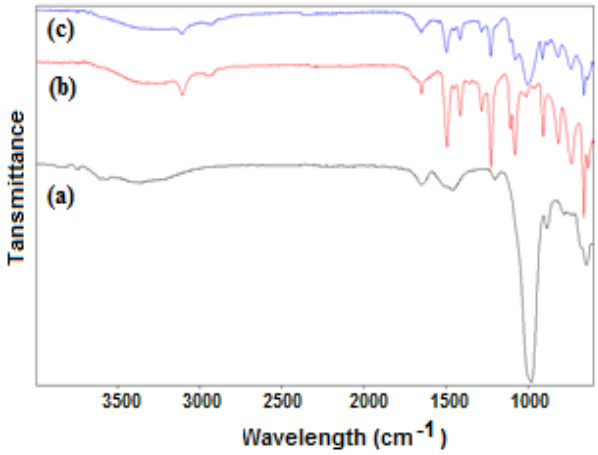

Figure 1. FTIR spectra of a) Sepiolite, b) PVI, and c) Sep-PVI composite.

In Figure 1a, the bands in the 4000–3000 cm^{-1} range is corresponding to Mg–OH bond vibrations[45], a band at 1655.06 cm^{-1} indicates the bending of zeolitic water, the bands in the 1200–600 cm^{-1} range is characteristic of silicate, the bands at 1202.83, 984.01 and 884.32 cm^{-1} can be attributed to the bonds of Si–O stretching vibration of the tetrahedral sheet[45,46] and the bands at 782.20, 682.52 and 646.05 cm^{-1} are related to Mg–OH bond vibrations (deformation at 782.20 cm^{-1} and bending at 682.52 and 646.05 cm^{-1}).[47,48] As shown in Figure 1b, the bands at 3106.57 cm^{-1} and 2953.40 cm^{-1} are corresponding to C–H (ring) and C–H (chain) stretching, respectively.[49] The bands appeared at 1497.02 cm^{-1}, 911.07 cm^{-1} and 816.24 cm^{-1} are correspond to C=N and

C=C stretching of imidazole rings, respectively. The absorption band at 660.64 cm^{-1} can be ascribed to bending vibration.[49,50]

For Sep-PVI sample (Figure 1c), the bands observed at 3111.44 and 821.11 cm^{-1} can be ascribed to the stretching vibration of the C–H and C=N of imidazole rings, respectively. The characteristic peaks of PVI were appeared in the spectrum of Sep-PVI composite, and confirmed that the composite has been produced.

4.1.2. XRD Analysis

The XRD patterns in the range of $2\theta = 5^{\circ}–50^{\circ}$ for the sepiolite, the Sep-PVI composite and PVI are given in Figure 2. Figure 2a shows that the characteristic diffraction peak of sepiolite was found in the diffraction pattern at about $2\theta = 6.966^{0}$ (110), related to the reflections of internal channel.[45] The d-spacing of the characteristic diffraction peaks for sepiolite (d_{110} = 12.68 nm) and Sep-PVI composite (d_{110} = 12.71 nm) are very similar. One main reason is that unlike smectite clays, sepiolite exhibits a structure where TOT layers are mightily bonded by covalent bonds. Another possible reason is that the silanol groups attended to the polymerization are mainly presented on the whole external surface of sepiolite.[52]

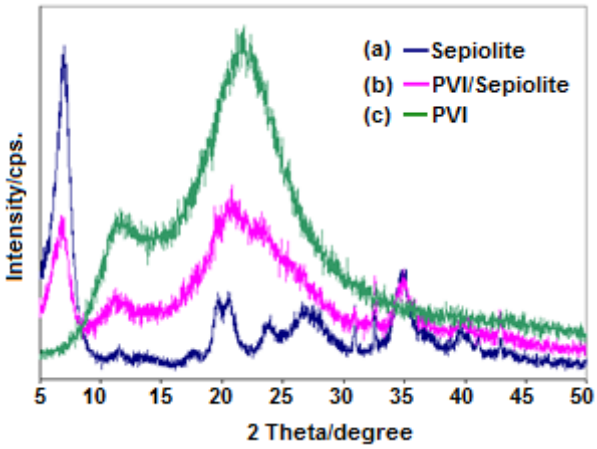

Figure 2. XRD patterns of the materials.

The diffraction intensity of Sep-PVI composite (Figure 2b) decreased when compared with sepiolite. The result was seen as an averment for substantially dispersion of sepiolite in PVI. Furthermore, some characteristic peaks of sepiolite were disappeared in the prepared composite. This may be ascribed to the homogenous dispersion of the sepiolite into PVI due to its bundles being generally delaminated to fiber sticks.[51-53]

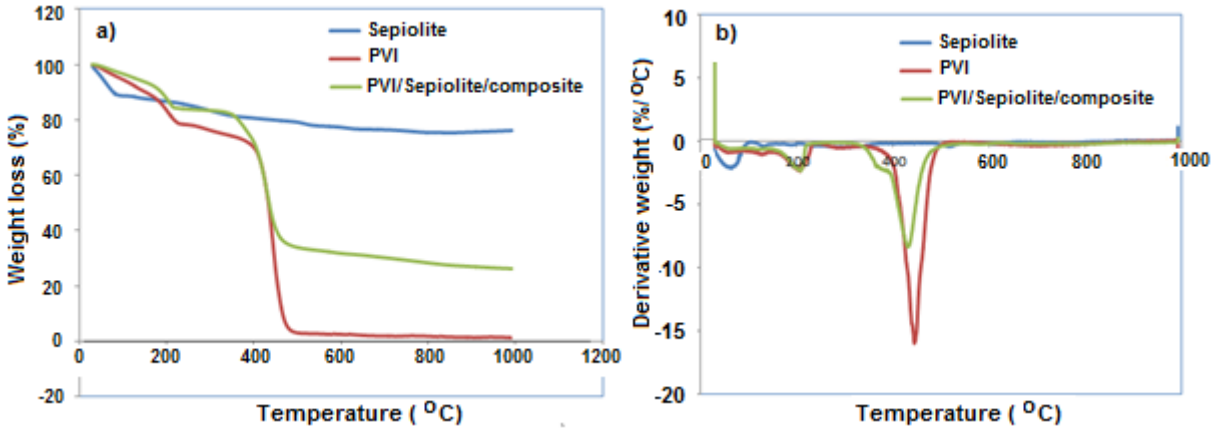

Figure 3. a) TGA, b) DTA curves of the materials.

4.1.3. TGA-DTA analysis

TGA and DTA curves of PVI, sepiolite and Sep-PVI composite are illustrated in Figure 3a and b. Figure 3a shows that the thermal decomposition of poly(vinylimidazole) is in one primary step and occurs in the temperature range of 340–500°C. In the TGA curve, the maximum of the decomposition temperature is determined at 450°C. The weight loss in the 340–500°C temperature range is ascribed to PVI chain's decomposition.[49,54,55] In the sepiolite thermogram, the primary and first weight loss is near 100°C due to loss of zeolitic water that it is physically bonded to sepiolite in the structural channels and on the external surface.[56] Two of the four coordinated crystallization water molecules and the other two molecules of sepiolite are lost at about 300°C and at 520°C, respectively.[46,57] Eventually, sepiolite lost hydroxyl groups or structural water around 750°C.[45] As can be seen from Figure 3a, the degradation temperature (429°C) of Sep-PVI composite prepared shifts to lower temperatures in compliance with PVI (444°C). The probable reason for these results may be

due to that the sepiolite catalyzes PVI degradation and/or the presence of sepiolite reducing the polymer chain stability via interparticular interactions.

4.1.4. SEM analysis

The surface morphology of the Sep-PVI composite was investigated by SEM analysis. Figure 4a-c shows the SEM images of sepiolite, PVI, and Sep-PVI composite respectively. SEM images in Figure 4a shows that sepiolite reveals stone-like aggregation. In SEM image of PVI, polymer showed spherical particulate structure. Additionally, PVI came into existence of particles with sizes < 2μm (Figure 4b). It can be seen from Figure 4c, that the prepared Sep-PVI composite has a smooth and dense surface and sepiolite shows a good dispersion in PVI. Furthermore the surface of sepiolite is covered with PVI. A good adhesion was found between the PVI and the sepiolite due to strong hydrogen bonding between the silanol groups of sepiolite and PVI[58] and the high surface area of the sepiolite.[59]

4.2. Effect of pH, initial concentration of Cu(II) ions and temperature on adsorption

The solution pH value makes a significant impact on the adsorption process due to protonation of functional groups in the adsorbent and the precipitation formation of heavy metal ions.[1–5,7,14] Considering the formation of Cu^{2+} hydroxide precipitate at higher pH values, the selected pH values in the batch experiments were set below 6.5 in this study. Also, the adsorption capacity of Sep-PVI composite for Cu^{2+} ions was investigated at the pH range of 2–6.5. It is found that the Cu^{2+} adsorption capacity of Sep–PVI composite increases with the initial pH increases from 2.0 to 6.5 and decreases when the initial pH is 6.0 (Figure is not shown). The optimal pH value for Cu^{2+} adsorption of by Sep–PVI composite is around 5. The imidazole groups of Sep–PVI composite are easily protonated at lower pH values, which means that more active sites are occupied by H^+ ions. When the initial solution pH value gradually increases, more active sites are deprotonated and the positive charge is reduced. This situation causes to a better affinity of the adsorbent to Cu(II) ions, resulting a higher adsorption capacity. Further as the pH value increases, hydroxide precipitate appears, and correspondingly the adsorption capacity declines. Thus, a pH value of 5 was selected for the following absorption studies.

The effect of different initial concentrations on adsorption of Cu(II) onto sepiolite and Sep-PVI composite is given in Figure 5. As can be seen in Figure 5, Cu(II) removal increases with an increase in the initial Cu(II) concentration. At higher Cu(II) concentration, this increase might be attributed to the increased contact probabilities between Cu(II) ions and the binding sites sites on the Sep-PVI composite.

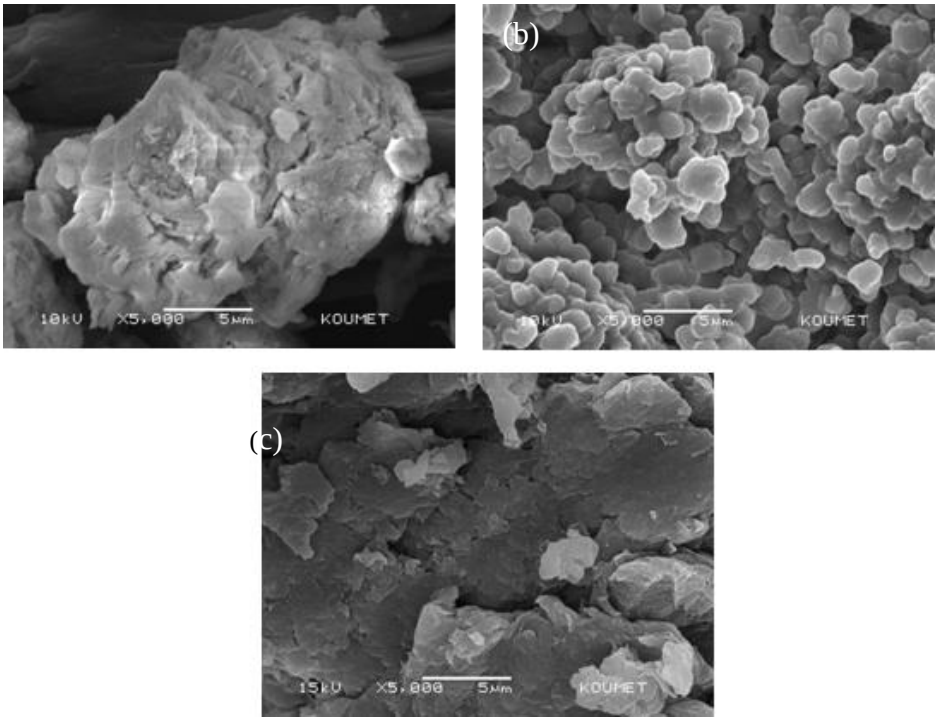

Figure 4. SEM photographs of: a) sepiolite, b) PVI and c) Sep-PVI composite.

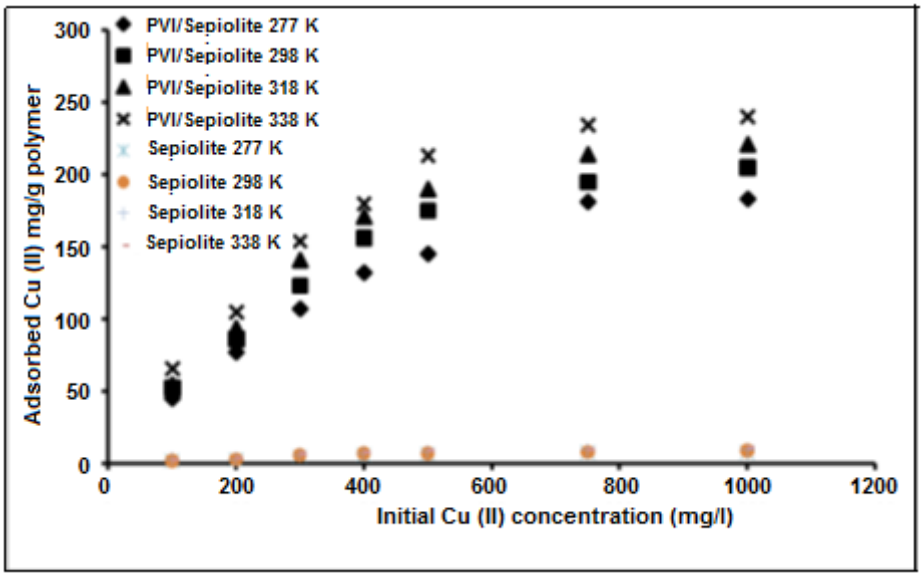

Figure 5. Effect of initial concentration of Cu(II) ions onto sepiolite and Sep-PVI composite.

In addition, the higher initial Cu(II) concentration provides an important driving force to overcome the mass transfer resistances between the Cu(II) aqueous solution and the Sep-PVI composite. As the binding sites are gradually occupied by Cu(II) ions, the adsorption process reaches the equilibrium. Also the Figure 5, for Cu(II) removal, shows that the adsorption capacity of prepared Sep-PVI composite is higher than that of sepiolite under the same adsorption conditions. The result can be explained with increase of the adsorption capacity of sepiolite for Cu(II) ions removal due to formation of composite with PVI. It is known that imidazole groups of PVI are complexed with divalent metallic ions catalyzed.[19]

The temperature effect on removal of Cu(II) ions by using sepiolite and Sep-PVI composite prepared was studied at different temperatures such as 277, 298, 318 and 338 K. The results obtained are shown in Figure 5. From this figure, it can be seen that the q_e values increase with increasing temperature. This situation may probably be attributed to higher collision frequencies at higher temperature.[60]

4.3. Nonlinear isotherm analysis for adsorption

The parameters of the adsorption isotherm model were obtained by using nonlinear regression using SPSS (Ver.17). The fourteen isotherm models were used in order to determine the characteristic parameters of the adsorption isotherm and predict the isotherms.

In the present study, the determination coefficient, R^2 was used to test the best-fitting isotherm to the experimental data:

$$R^2 = \frac{\sum_{i=1}^{n}\left(q_{meas} - \overline{q_{calc}}\right)^2}{\sum_{i=1}^{n}\left(q_{meas} - \overline{q_{calc}}\right)^2 + \sum_{i=1}^{n}\left(q_{meas} - q_{calc}\right)^2} \qquad (16)$$

In this equation, q_{calc} is the calculated the equilibrium solid phase concentration, $\overline{q_{calc}}$ is the average of q_{calc} and q_{meas} is the measured concentration of the equilibrium solid phase. If $R^2 = 1$, the fit is perfect for all points.

4.3.1. Single- and two-parameter isotherm models

The parameters of single- and two-parameter isotherm models are presented in Table 1. Figure 6 shows the predicted and experimental the single- and two-parameter isotherms by non-linear method for the adsorption of Cu(II) onto Sep-PVI composite.

Among the isotherm models, Henry's law has a single-parameter model and is the simplest one. Henry's law is feasible only in the lower range of adsorbate concentration.

Table 1. Isotherm parameters for the adsorption of Cu(II) onto Sep-PVI composite obtained by non-linear methods (single- and two-parameter isotherms)

Isotherm model	Equations	Equation No	Parameters			
			277 K	298 K	318 K	338 K
Henry	$q_e = K_{HE} C_e$	(2)	K_{HE} = 0.299 R^2 = 0.834	K_{HE} = 0.347 R^2 = 0.773	K_{HE} = 0.388 R^2 = 0.738	K_{HE} = 0.436 R^2 = 0.738
Freunlich	$q_e = K_F C_e^{1/n}$	(3)	K_F = 9.8 n = 2.23 R^2 = 0.947	K_F = 14.55 n = 2.45 R^2 = 0.918	K_F = 18.25 n = 2.58 R^2 = 0.901	K_F = 24.24 n = 2.79 R^2 = 0.914
Langmuir	$q_e = \frac{q_m K_L C_e}{(1 + K_L C_e)}$	(4)	K_L = 0.00404 q_m = 247.52 R^2 = 0.990	K_L = 0.00525 q_m = 261.91 R^2 = 0.982	K_L = 0.00613 q_m = 277.84 R^2 = 0.981	K_L=0.00744 q_m = 291.93 R =0.978
Dubinin-Radushkevich	$q_e = q_m \exp\left(-B[RT\ln(1+1/C_e)]^2\right)$	(5)	B = 0.000728 q_m = 144.3 R^2 = 0.719	B = 0.000469 q_m = 162.9 R^2 = 0.722	B = 0.000375 q_m = 179.83 R^2 = 0.758	B = 0.00017 q_m = 190.78 R^2 = 0.663
Temkin	$q_e = \frac{RT}{b}\ln(K_T C_e) = B_1 \ln(K_T C_e)$	(6)	K_T = 0.0366 B_1 = 56.24 R^2 = 0.982	K_T = 0.0473 B_1 = 59.35 R^2 = 0.969	K_T = 0.0544 B_1 = 62.87 R^2 = 0.965	K_T = 0.0801 B_1 = 61.72 R^2 = 0.961
Halsey	$q_e = (K_H C_e)^{1/n_H}$	(7)	K_H = 162.34 n_H = 2.23 R^2 = 0.947	K_H = 706.34 n_H = 2.45 R^2 = 0.918	K_H = 1795 n_H = 2.58 R^2 = 0.901	K_H = 7291.9 n_H = 2.79 R^2 = 0.914

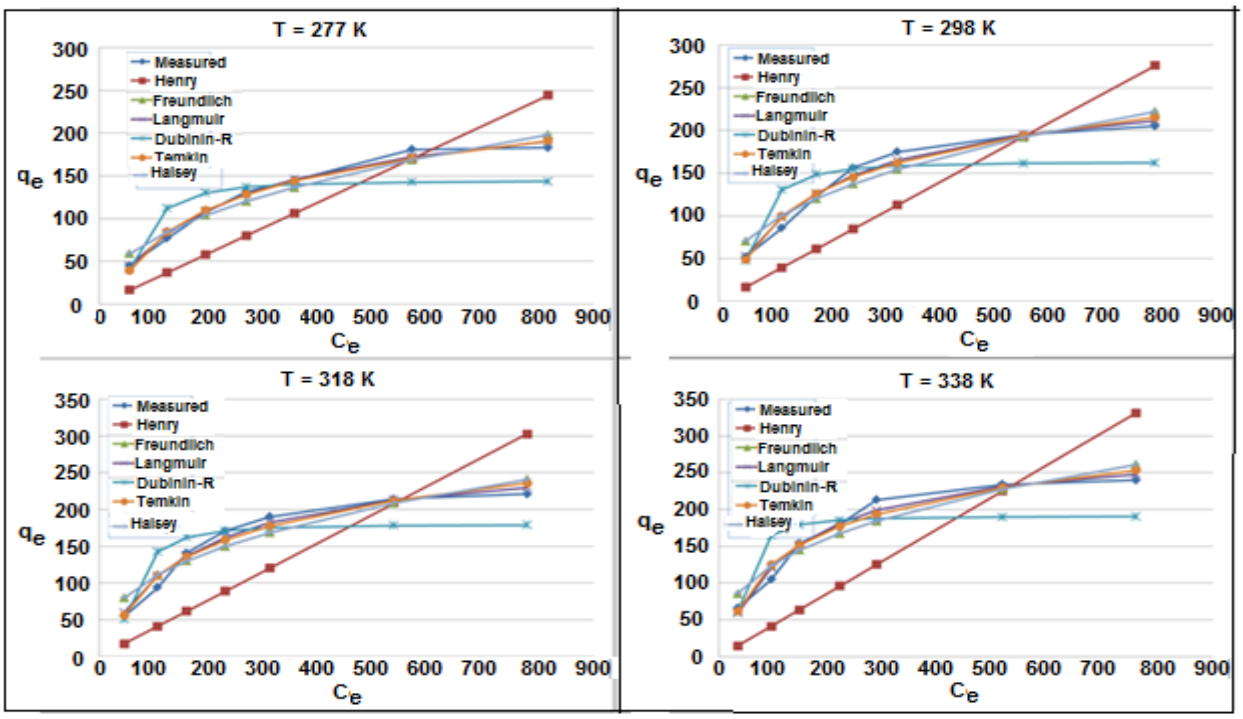

Figure 6. Single- and two-parameter isotherms obtained using the non-linear methods for the adsorption of Cu(II) onto Sep-PVI composite.

Therefore, it can be seen from Figure 6 and Table 1 that this model (R^2 varies from 0.738 to 0.834) completely fails to predict the adsorption equilibrium isotherm in this study.

For two-parameter isotherm models, the Langmuir isotherm model (R^2 varies from 0.978 to 0.990) provides a good fit to the experimental data for all temperatures whereas the Freundlich, Dubinin-Radushkevich, Temkin and Halsey values are considerably lower. The Langmuir equation is given in Eq. (4) (Table 1) where, q_m (mg g^{-1}) is the monolayer adsorption capacity of the composite, q_e (mg g^{-1}) is the equilibrium adsorption capacity, K_L (L g^{-1}) is the Langmuir constant related to the enthalpy of adsorption which is calculated by using the van't Hoff equation, and C_e is the equilibrium concentration (mg l^{-1}) of Cu(II).[61] It can be deduced that surface of Sep-PVI composite is homogenous for the adsorption of Cu(II) ions by monolayer adsorption and all adsorption sites are equal. As shown in Table 1, the maximum adsorption values are 247.52, 261.91, 277.84 and 291.93 mg g^{-1} at 277, 298, 318 and 338 K, respectively. The parameter K_L is related to the affinity of adsorbate–adsorbent.[62] K_L represents the equilibrium adsorption constant.[63] It was found that the adsorption process was more favorable at higher temperatures, and hereby the process is endothermic. According to the results, the best-fitted adsorption isotherm models were in the order: Langmuir > Temkin > Freundlich = Halsey > Dubinin-Radushkevich.

4.3.2. Three-, four- and five-parameter isotherm models

The parameters of three-, four- and five-parameter isotherm models are presented in Table 2. Figure 7 shows the predicted and experimental the three-, four- and five-parameter isotherms by non-linear methods for the adsorption of Cu(II) onto Sep-PVI composite. The Khan and Toth isotherms have similar and high determination coefficients when compared to Radke-Prausnitz, Sips, Koble-Corrigan and Redlich-Peterson isotherms (Table 2). Although the R^2 values of the Khan isotherm model is satisfactory (0.986 to 0.995), the predicted values of q_m by the isotherm model do not match the experimental equilibrium data (Figure 7). Therefore, the Toth isotherm shows a better fit to the adsorption data for the adsorption of Cu(II). The coefficients of correlation of the Toth isotherm model are good (R^2 varied from 0.981 to 0.994) for all the tested systems. The order of the equilibrium constant, b_T, of Toth isotherm is similar to the equilibirium constant parameter K_L of Langmuir. Therefore, Toth isotherm model is better precise for the experimental equilibrium data compared to other three-parameter isotherm models

.

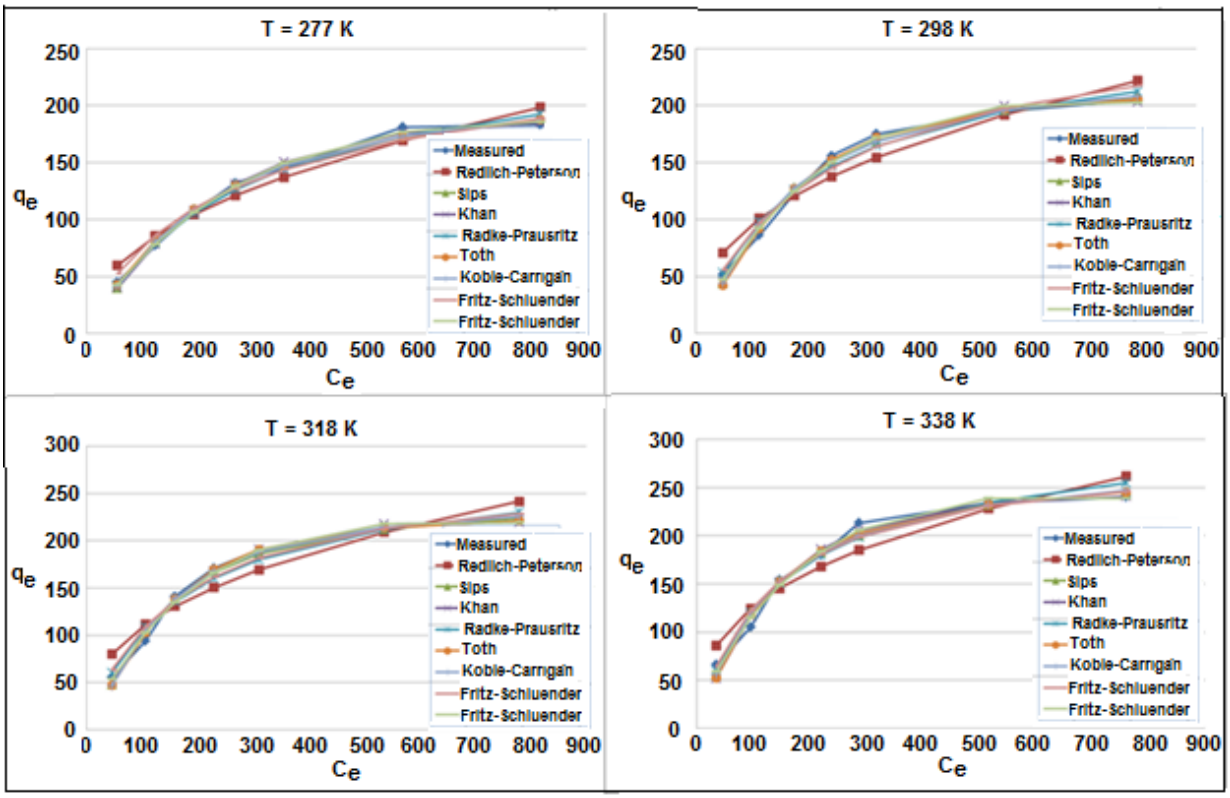

Figure 7. Three-, four- and five-parameter isotherms obtained using the non-linear methods for the adsorption of Cu(II) onto Sep-PVI composite

Table 2. Isotherm parameters for the adsorption of Cu(II) onto Sep-PVI composite obtained by non-linear methods (three-, four- and five-parameter isotherms)

Isotherm model	Equations	Equation No	Parameters			
			277 K	298 K	318 K	338 K
Redlich-Peterson	$q_e = \frac{K_R C_e}{1 + a_{RP} C_e^{\beta}}$	(8)	K_R = 75.9 a_{RP} = 7.39 β = 0.56 R^2 = 0.949	K_R = 109.9 a_{RP} = 7.26 B = 0.598 R^2 = 0.919	K_R = 131.48 a_{RP} = 7.01 β = 0.616 R^2 = 0.903	K_R = 161.71 a_{RP} = 6.48 β = 0.646 R^2 = 0.915
Sips	$q_e = q_m \frac{(K_S C_e)^{\gamma}}{1 + (K_S C_e)^{\gamma}}$	(9)	q_m = 225.3 K_S = 0.00489 γ = 1.173 R^2 = 0.992	q_m = 233.9 K_S = 0.00655 γ = 1.263 R^2 = 0.987	q_m = 244.17 K_S = 0.00774 γ = 1.333 R^2 = 0.99	q_m = 281.2 K_S = 0.00806 γ = 1.081 R^2 = 0.979
Khan	$q_e = \frac{q_m b_K C_e}{(1 + b_K C_e)^{a_K}}$	(10)	q_m = 729.2 b_K = 0.00113 a_K = 1.98 R^2 = 0.995	q_m = 880.5 b_K = 0.00122 a_K = 2.12 R^2 = 0.992	q_m = 878.9 b_K = 0.00149 a_K = 2.00 R^2 = 0.993	q_m = 569.2 b_K = 0.0031 a_K = 1.42 R^2 = 0.986
Radke-Prausnitz	$q_e = \frac{a_R r_R C_e^{\beta_R}}{a_R + r_R C_e^{\beta_R - 1}}$	(11)	a_R = 238.28 r_R = 0.94 β_R = 0.01143 R^2 = 0.988	a_R = 231.72 r_R = 1.41 β_R = 0.0183 R^2 = 0.980	a_R = 229.5 r_R = 1.75 β_R = 0.028 R^2 = 0.977	a_R = 212.91 r_R = 2.28 β_R = 0.051 R^2 = 0.974
Toth	$q_e = \frac{q_m b_T C_e}{\left(1 + (b_T C_e)^{n_T}\right)^{1/n_T}}$	(12)	q_m = 224.11 b_T = 0.00392 n_T = 1.219 R^2 = 0.992	q_m = 215.34 b_T = 0.00416 n_T = 1.965 R^2 = 0.992	q_m = 227.21 b_T = 0.0047 n_T = 2.132 R^2 = 0.994	q_m = 267.38 b_T = 0.00633 n_T = 1.332 R^2 = 0.981
Koble-Carrigan	$q_e = \frac{A_{KC} B_{KC} C_e^{n_{KC}}}{1 + B_{KC} C_e^{n_{KC}}}$	(13)	A_{KC} = 229.6 B_{KC} = 0.00234 n_{KC} = 1.131 R^2 = 0.992	A_{KC} = 234.8 B_{KC} = 0.00177 n_{KC} = 1.26 R^2 = 0.987	A_{KC} = 245.1 B_{KC} = 0.00125 n_{KC} = 1.373 R^2 = 0.99	A_{KC} = 283.7 B_{KC} = 0.00571 n_{KC} = 1.07 R^2 = 0.979
Fritz-Schluender	$q_e = \frac{A C_e^{\alpha_{FS}}}{1 + B_{FS} C_e^{\beta_{FS}}}$	(14)	A = 2.5 B_{FS} = 0.0083 α_{FS} = 0.81 β_{FS} = 0.82 R^2 = 0.986	A = 2.7 B_{FS} = 0.0052 α_{FS} = 0.82 β_{FS} = 0.89 R^2 = 0.973	A = 3.35 B_{FS} = 0.00327 α_{FS} = 0.805 β_{FS} = 0.97 R^2 = 0.98	A = 4.18 B_{FS} = 0.00577 α_{FS} = 0.817 β_{FS} = 0.934 R^2 = 0.98
Fritz-Schluender	$q_e = \frac{\alpha_1 C_e^{\beta_1}}{\alpha_1' + \alpha_2 C_e^{\beta_2}}$	(15)	α_1 = 107.9 α_1' = 59.1 α_2 = 0.00223 β_1 = 0.793 β_2 = 1.519 R^2 = 0.996	α_1 = 145.9 α_1' = 79.5 α_2 = 0.00712 β_1 = 0.847 β_2 = 1.464 R^2 = 0.993	α_1 = 113.3 α_1' = 51.22 α_2 = 0.0066 β_1 = 0.845 β_2 = 1.433 R^2 = 0.993	α_1 = 285.14 α_1' = 53.80 α_2 = 0.00257 β_1 = 0.686 β_2 = 1.515 R^2 = 0.99

As can also be seen from Table 2, Fritz-Schlunder (four-parameter) model unable to describe the data because of low determination coefficients, compared to Fritz-Schlunder (five-parameter) model. The high determination coefficients (R^2 varies from 0.990 to 0.996) for Fritz-Schlunder (five-parameter) model were obtained for the all studied systems. As a result, the increased number of constants in the isotherm model equations would be able to simulate the model variations more accurately. However, the maximum capacities of

adsorption determined using the Fritz-Schlunder (five-parameter) model was compared to experimental data and it was found that the values are lower than those for the Langmuir and Toth isotherm models.

4.4. Adsorption thermodynamics

The van't Hoff equation can be used to determine the thermodynamic parameters because of temperature dependence of the equilibrium constant (K_L). This equation can be integrated as:[61]

$$\ln K_L = \frac{\Delta S^0}{R} - \frac{\Delta H^0}{R}\left(\frac{1}{T}\right) \quad (17)$$

in this equation, R is the universal gas constant (J mol^{-1} K^{-1}) and T the absolute temperature (K). ΔS° and ΔH° are the entropy and enthalpy changes of the adsorption process. They were determined from the intercept and slope of the plot of ln K_L versus $1/T$, respectively (Figure 8).

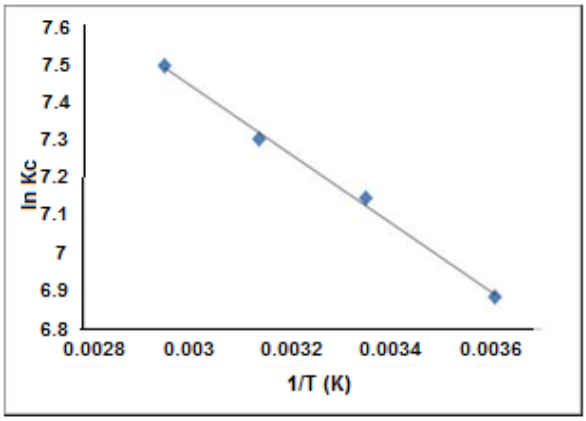

Figure 8 The plot of *ln* K_L versus *1/T* for the determination of the thermodynamic parameters for the adsorption of Cu(II) onto Sep-PVI composite.

The equation of free energy for all studied temperature is obtained as:[61]

$$\Delta G^0 = \Delta H^0 - T\Delta S^0 \quad (18)$$

From Eq. (18), the Gibbs free energy change (*ΔG°*) was calculated as -15.869, -17.651, -19.348 and -21.045 kJ mol^{-1} at 277, 298, 318, and 338 K, respectively (Table 3). According to the negative *ΔG°* values, the adsorption process is spontaneous and thermodynamically feasible. ΔG° values change usually between −20 and 0 kJ mol^{-1} for physisorption, whereas the values are often in the range of −80 to −400 kJ mol^{-1} for chemisorption.[64] In this study, the *ΔG°* values obtained indicate that the adsorption is physisorption. The enthalpy (*ΔH°*) and entropy (*ΔS°*) changes were calculated as +84,853 J mol^{-1} K^{-1} and +7,635 kJ mol^{-1}, respectively (Table 3).

The *ΔH°* has positive value, which indicates endothermic adsorption process. From positive value of *ΔS°*, it can be said that the randomness at the solid-solute interface increases during the adsorption process.

Table 3. The thermodynamic values of the Cu(II) adsorption onto Sep-PVI composite at different temperatures

Temperature (K)	ΔG^0 (kJ mol^{-1})	ΔH^0 (kJ mol^{-1})	ΔS^0 (J mol^{-1} K^{-1})
277	-15.869	+7.635	+84.853
298	-17.651		
318	-19.348		
338	-21.045		

4.5. Comparison of the adsorption capacities of different adsorbents for Cu(II)

For Cu(II) removal, a summary of the adsorption capacities of other adsorbents in the literature and Sep-PVI composite are given in Table 4. As can be seen from Table 4 that the maximum adsorption capacity of the Sep-PVI composite prepared in this study is found as 261.91 mg g^{-1}. The value is much higher than those of other adsorbents. These results indicate that the Sep-PVI composite synthesized is a promising adsorbent for removal of the Cu(II) ions from aqueous solutions.

5. CONCLUSIONS

A novel Sep-PVI composite for the removal of Cu(II) ions were prepared by in-situ polymerization from sepiolite and 1-vinyl imidazole. The obtained composite was characterized by XRD, FTIR, TGA and SEM. The removal of Cu(II) ions onto the Sep-PVI composite was studied at different temperatures, and the equilibrium data were modelled using Henry's law, Langmuir, Freundlich, Temkin, Dubinin-Radushkevich, Halsey, Redlich-Peterson, Khan, Sips, Radke-Prausnitz, Koble-Corrigan, Toth, Fritz and Schlunder (four-parameter) and Fritz and Schlunder (five-parameter) isotherm models. Among two-parameter models, the Langmuir model better described the isotherm data with high R^2. In the case of three-parameter models, the Toth model was found to provide closest fit to the equilibrium experimental data even better than Langmuir model. The maximum adsorption capacity of Sep-PVI composite was in very well consistent with the experimental data. The high determination coefficients for Fritz-Schlunder (five-parameter) model were obtained for the all studied systems. However, the maximum capacity of adsorption determined using the Fritz-Schlunder (five-parameter) model was compared to experimental data and it was found that the values were lower than those of the

Table 4. Comparison of the adsorption properties of various adsorbents for the removal of Cu(II)

Adsorbents	T (°C)	pH	q_m (mg g^{-1})	Ref.
Crosslinked chitosan-coated bentonite beads	25	4.0	9.43	(3)
Non-crosslinked chitosan-coated bentonite beads	25	4.0	12.21	(3)
Chitosan–zeolite composites (CZ-2)	25	5.0	14.75	(13)
Chitosan–zeolite composites (CZ-0)	25	3.0	25.61	(13)
Chitosan–zeolite composite	25	3.0	25.96	(4)
Chitosan-tripolyphosphate beads	27	4.5	26.06	(9)
EDTA functionalized Fe_3O_4 magnetic nano-particles	25	6.0	46.27	(5)
Chitosan–zeolite composites (CZ-1)	25	3.0	51.32	(13)
Sulfonated magnetic graphene oxide composite	30	5.0	56.86	(15)
Poly(N-isopropylacryl amide-co-acrylic acid) hydrogels	30	5.0	67.25	(7)
PVA/silica/MPTMS	25	6.0	70.01	(14)
Humic acid-immobilized polymer/bentonite composite	30	5.0	106.2	(16)
Fish bones	20	4.5	124.5	(1)
Mesoporous adsorbents prepared with fly ash	20	4.5	221	(2)
Sep-PVI composite	25	5.0	261.91	In this study

Langmuir and Toth isotherm models. Additionally, the study reveals that the more isotherm parameters provide a better fitting of the adsorption equilibrium data. Adsorption capacity of Sep-PVI composite for Cu(II) increased with an increase in temperature from 277 to 338 K, indicating an endothermic adsorption. Adsorption experiments showed that Sep-PVI composite was an effective adsorbent and could be used for the removal of Cu(II) from wastewater.

ACKNOWLEDGEMENTS

Authors thank to Kocaeli University and Uludağ University for continuous motivation. The authors also thank to METU Central Laboratory for analytical characterization support.

Nomenclature

a_K	Khan model exponent
a_R	Radke-Prausnitz isotherm constant
a_{RP}	Redlich-Peterson model constant, l mg^{-1}
A	Fritz-Schlunder four-parameter model constant
A_{KC}	Koble-Carrigan isotherm constant
b_K	Khan isotherm constant
b_T	Toth isotherm constant
B	Heat of adsorption constant, J mol^{-1}
B_1	Constant in Temkin adsorption isotherm, J mol^{-1}
B_{FS}	Constant in Fritz-Schlunder four-parameter model
B_{KC}	Koble-Carrigan isotherm constant
C_e	Equilibrium concentration of adsorbate in solution, mg l^{-1}
E	Mean free energy, kJ mol^{-1}
K_F	Freundlich isotherm constant, $mg^{1-(1/n)}$ $l^{1/n}$ g^{-1}
K_{HE}	Henry's law constant, l mg^{-1}
K_H	Halsey isotherm constant
K_L	Langmuir isotherm equilibrium binding constant, l mg^{-1}
K_R	Redlich-Peterson isotherm constant, l mg^{-1}
K_S	Sips isotherm constant, l mg^{-1}
K_T	Temkin isotherm constant
n	Exponent in Freundlich isotherm
n_H	Halsey equation exponents
n_{KC}	Koble−Carrigan model exponent
n_T	Toth model exponent
q_e	Amount of adsorption at equilibrium, mg g^{-1}
q_m	Maximum adsorption capacity, mg g^{-1}
r_R	Radke-Prausnitz isotherm constant
R	Universal gas constant, 8.314 J mol^{-1} K^{-1}
R^2	Correlation coefficient
T	Absolute temperature, K
α	Radke-Prausnitz isotherm constant
α_1	Fritz-Schlunder five-parameter model sorption capacity, mg g^{-1}
α'_1	Fritz-Schlunder five-parameter model constant
α_2	Fritz-Schlunder five-parameter model constant
α_{FS}	Fritz-Schlunder four-parameter model exponent
β	Constant in Dubinin-Radushkevich model
β_1	Fritz-Schlunder five-parameter model exponent
β_2	Fritz-Schlunder five-parameter model exponent
β_{FS}	Fritz-Schlunder four-parameter model exponent
β_R	Radke-Prausnitz model exponent
β_{RP}	Redlich-Peterson isotherm constant
ε	Polanyi potential
γ	Sips model exponent

Conflict of interest

Authors declare that there is no a conflict of interest with any person, institute, and company, etc.

REFERENCES

1. Kizilkaya, B.; Tekinay, A. A.; Dilgin, Y. *Desalination* **2010**, 264, 37–47.

2. Wu, X.-W.; Ma, H.-W.; Zhang, L.-T.; Wang, F.-J. *Appl. Surf. Sci.* **2012**, 261, 902– 907.

3. Dalida, M.L.P.; Mariano, A.F.V.; Futalan, C.M.; Kan, C.-C.; Tsai, W.-C.; Wan, M.-W. *Desaliation* **2011**, 275, 154–159.

4. Wan Ngah, W.S.; Teong, L.C.; Toh, R.H.; Hanafiah, M.A.K.M. *Chem. Eng. J.* **2012**, 209, 46–53.

5. Liu, Y.; Chen, M.; Hao, Y. *Chem. Eng. J.* **2013**, 218, 46–54.

6. Pellera, F.-M.; Giannis, A.; Kalderis, D.; Anastasiadou, K.; Stegmann, R.; Wang, J.-Y.; Gidarakos, E. *J. Environ. Manag.* **2012**, 96, 35–42.

7. Chen, J.J.; Ahmad, A.L.; Ooi, B.S. *J. Environ. Chem. Eng.* **2013**, 1, 339–348.

8. Karapinar, N.; Donat, R. *Desalination* **2009**, 249, 123–129.

9. Wan Ngah, W.S.; Fatinathan, S. *J. Environ. Manag.* **2010**, 91, 958–969.

10. Serencam, H.; Ozdes, D.; Duran, C.; Senturk, H.B. *Desalin. Water Treat.* **2014**, 52, 3226–3236.

11. Ibrahim, H.S.; Ammar, N.S.; Ghafar, H.H.A.; Farahat, M. *Desalin. Water Treat.* **2012**, 48, 320–328.

12. Nadaroglu, H.; Kalkan, E.; Demir, N. *Desalination* **2010**, 251, 90–95.

13. Wan Ngah, W.S.; Teong, L.C.; Toh, R.H.; Hanafiah, M.A.K.M. *Chem. Eng. J.* **2013**, 223, 231–238.

14. Keshtkar, A.R.; Irani, M.; Moosavian, M.A. *J. Taiwan Inst. Chem. Eng.* **2013**, 44, 279–286.

15. Hu, X.-J.; Liu, Y.-G.; Wang, H.; Chen, A.-W.: Zeng, G.-M.; Liu, S.-M.; Guo, Y.-M.; Hu, X.; Li, T.-T.; Wang, Y.-Q.; Zhou, L.; Liu, S.-H. *Sep. Purif. Technol.* **2013**, 108, 189–195.

16. Anirudhan, T.S.; Suchithra, P.S. *Chem. Eng. J.* **2010**, 156, 146–156.

17. Yu, Y.; Qi, S.; Zhan, J.; Wu, Z.; Yang, X.; Wu, D. *Mater. Res. Bull*. **2011**, 46, 1593–1599.

18. Kavas, H.; Baykal, A.; Senel, M.; Kaynak, M. *Mater. Res. Bull.* **2013**, 48, 3973–3980.

19. Tekin, N.; Kadıncı, E.; Demirbaş, Ö.; Alkan, M.; Kara, A. *J. Colloid Interf. Sci*. **2006**, 296, 472–479.

20. Gurbuz, O.; Sahan, Y.; Kara, A.; Osman, B. *Hacettepe J. Biol. Chem*. **2009**, 37, 353–357.

21. Caner, H.; Yilmaz, E.; Yilmaz, O. *Carbohyd. Polym.* **2007**, 69, 318–325.

22. Bergaya, F.; Jaber, M.; Lambert, J. F.; Galimberti, M. *Rubber-Clay Nanocomposites: Science, Technology, and Applications. (1. Clay and Clay Minerals).* Wiley, 2011.

23. Fukushima, K.; Tabuani, D.; Camino, G. *Mater. Sci. Eng. C*. **2009**, 29, 1433–1441.

24. Kara, A.; Demirbel, E.; Sözeri, H.; Küçük, İ.; Ovalıoğlu, H. *Hacettepe J. Biol. Chem.* **2014**, 42, 299–312.

25. Ho, Y.S. *Carbon* **2004**, 42, 2115–2116.

26. Kumar, K.V. *J. Hazard. Mater. B.* **2006**,136, 197–202.

27. Tekin, N.; Kaya, A.U.; Esmer, K.; Kara, A. *Appl. Clay Sci.* **2012**, 57, 32–38.

28. Al-Degs, Y.S.; Abu-El-Halawa, R.; Abu-Alrub, S.S. *Chem. Eng. J.* **2012**, 191, 185– 194.

29. Freundlich, H.M.F. *Z. Phys. Chem.* **1906**, 57, 385–471.

30. Rengaraj, S.; Yeon, J.-W.; Kim, Y.; Jung, Y.; Ha, Y.-K.; Kim, W.-H. *J. Hazard. Mater.* **2007**, 143, 469–477.

31. Langmuir, I. *J. Am. Chem. Soc.* **1916**, 38, 2221–2295.

32. Dubinin, M.M. *Chem. Rev.* **1960**, 60, 235–266.

33. Kundu, S.; Gupta, A.K. *Chem. Eng. J.* **2006**, 122, 93–106.

34. Halsey, G. *J. Chem. Phys.* **1948**, 16, 931-937.

35. Redlich, O.; Peterson, D.L. *J. Phys. Chem.* **1959**, 63, 1024.

36. Sips, R.J. *J. Chem. Phys*. **1948**, 16, 490–495.

37. Foo, K.Y.; Hameed, B.H. *Chem. Eng. J.* **2010**, 156, 2–10.

38. Khan, A.R.; Ataullah, R.; Al-Haddad, A. *J. Colloid Interf. Sci.* **1997**, 194, 154–165.

39. Liu, Y.; Liu, Y.-J. *Sep. Purif. Technol*. **2008**, 61, 229–242.

40. Vijayaraghavan, K.; Padmesh, T.V.N.; Palanivelu, K.; Velan, M. *J. Hazard. Mater. B*. **2006**, 133, 304–308.

41. Toth, J. *Acta Chem. Acad. Sci. Hungaria*. **1971**, 69, 311–317.

42. Koble, R.A.; Corrigan, T.E. *Ind. Eng. Chem.* **1952**, 44, 383–387.

43. Basha, S.; Murthy, Z.V.P.; Jha, B. *Ind. Eng. Chem. Res.* **2008**, 47, 980–986.

44. Fritz, W.; Schlunder, E.U. *Chem. Eng. Sci.* **1974**, 29, 1279–1282.

45. Rangabhashiyam, S.; Anu, N.; Nandagopal, M.S.G.; Selvaraju, N. *J. Environ. Chem. Eng.* **2014**, 2, 398–414.

46. Beauger, C.; Lainé, G.; Burr, A.; Taguet, A.; Otazaghine, B.; Rigacci, A. *J. Membr. Sci.* **2013**, 130, 167–179.

47. Alkan, M.; Tekin, G.; Namli, H. *Micropor. Mesopor. Mat.* **2005**, 84, 75–83.

48. Wan, C.; Chen, B. *Nanoscale.* **2011**, 3, 693–700.

49. Unal, H. I.; Erol, O.; Gumus, O.Y. *Colloids and Surfaces A: Physicochem. Eng. Aspects.* **2014**, 442, 132–138.

50. Chen, Z.; Yang, J.; Yin, D.; Li, Y.; Wu, S.; Lu, J.; Wang, J. *J. Membrane Sci.* **2010**, 349, 175–182.

51. Soheilmoghaddam, M.; Wahit, M.U.; Yussuf, A.A.; Al-Saleh, M.A.; Whye, W.T. *Polym. Test.* **2014**, 33, 121–130.

52. Lu, P.; Xu, J.; Liu, K. *J. Appl. Polym. Sci.* **2011**, 119, 3043–3050.

53. Killeen, D.; Frydrych, M.; Chen, B. *Mater. Sci. Eng. C*. **2012**, 32, 749-757.

54. Jang, J.; Kim, H. *J. Appl. Polym. Sci.* **1995**, 56, 1495–1504.

55. Fodor, C.; Bozi, J.; Blazsoi, M.; Ivain, B. *Macromolecules* **2012**, 45, 8953–8960.

56. Frost, R.L.; Kristof, J.; Horvath, E. *J. Therm. Anal. Calorim.* **2009**, 98, 749–755.

57. Serna, C.; Ahlrichs, J.L.; Serratosa, J.M. *Clay Miner*. **1975**, 23, 452–457.

58. Tartaglione, G.; Tabuani, D.; Camino, G.; Moisio, M. *Compos. Sci. Technol*. **2008**, 68, 451–460.

59. Bidsorkhi, H.C.; Soheilmoghaddam, M.; Pour, R.H.; Adelnia, H.; Mohamad, Z. *Polym. Test.* **2014**, 37, 117–122.

60. Ghasemi, Z.; Seif, A.; Ahmadi, T.S.; Zargar, B.; Rashidi, F.; Rouzbahani, G.M. *Adv. Powder Technol.* **2012**, 23, 148–156.

61. McKay, G.; Mesdaghinia, A.; Nasseri, S.; Hadi, M.; Aminabad, M.S. *Chem. Eng. J.* **2014**, 251, 236–247.

62. Oubagaranadin, J.U.K.; Murthy, Z.V.P. *Appl. Clay Sci.* **2010**, 50, 409–413.

63. Kumar, K.V. *Dyes Pigments.* **2007**, 74, 595–597.

64. Özcan, A.; Ömeroğlu, Ç.; Erdoğan, Y.; Özcan, A.S. *J. Hazard. Mater.* **2007**, 140, 173–179.

ORCID

0000-0002-9390-9875 (A. Kara)

0000-0003-3560-2995 (M. Kılıç)

0000-0003-0141-5817 (N. Dinibütün)

0000-0003-0141-5817 (A. Şafaklı)